Temperature climatology of the middle atmosphere from long-term lidar measurements at mid- and low-latitudes.

I. Stuart McDermid, Thierry Leblanc
Jet Propulsion Laboratory, California Institute of Technology, Table Mountain Facility, Wrightwood, CA 92397
mcdermid@tmf.jpl.nasa.gov, Tel: +1 760 249 4262, Fax: +1 760 249 5392

Philippe Keckhut, Alain Hauchecorne
Service d'Aéronomie du CNRS, 91371 Verrières-le-Buisson, France

C. Y. She and David A. Krueger
Department of Physics Colorado State University Fort Collins, CO 80523

1. Introduction

The temperature structure of the middle atmosphere has been studied for several decades using a variety of techniques. However, temperature profiles derived from lidar measurements can provide improved vertical resolution and accuracy [*Hauchecorne and Chanin*, 1980]. Lidars can also provide long-term data series relatively absent of instrumental drift, and integration of the measurements over several hours removes most of the gravity wave-like short-scale disturbances.

This paper describes a seasonal climatology of the middle atmosphere temperature derived from lidar measurements obtained at several mid- and low-latitude locations. Results from the following lidars, which have all obtained a long-term measurement record, were used in this study: the two Rayleigh lidars of the Service d'Aéronomie du CNRS, France, located at the Observatoire de Haute Provence (OHP, 44.0°N) and at the Centre d'Essais des Landes (CEL, 44.0°N), the two Rayleigh/Raman lidars of the Jet Propulsion Laboratory, USA, located at Table Mountain, California (TMF, 34.4°N) and at Mauna Loa, Hawaii (MLO, 19.5°N), and the Colorado State University, USA, sodium lidar located at Fort Collins, Colorado (CSU, 40.6°N). The overall data set extends from 1978 to 1997 with different periods of measurements depending on the instrument. Three of the instruments are located at primary or complementary stations (OHP, TMF, MLO) within the Network for Detection of Stratospheric Change (NDSC). Several aspects of the temperature climatology obtained by lidar in the middle atmosphere are presented, including the climatological temperature average through the year; the annual and semi-annual components, and the differences compared to the CIRA-86 climatological model.

2. The instruments, database and data processing.

The Rayleigh/Raman and sodium fluorescence lidar techniques for measuring temperature profiles are well established and have been described in detail by numerous authors. Some details of the lidar techniques used in this study can be found in *Hauchecorne and Chanin* [1980], *Leblanc et al.* [1998a], *She et al.* [1992], *McDermid et al.* [1995].

At mid-latitudes the CNRS-SA Rayleigh lidar at OHP (44.0°N, 6.0°E) has obtained more than 1240 nighttime temperature profiles between 30 and 95 km from 1978 to the present with 75 to 300 m vertical resolution, and 670 profiles at CEL (44.0°N, 1.0°W) from 1986 to 1994 with 300 m vertical resolution. The total estimated error at the top of each profile is about 20-25 K. This error drops to less than 1 K at mid-range (typically 55 km) and below. The CSU (40.6°N, 105.1°W) Na lidar has obtained nearly 250 temperature profiles in the Na layer between 80 and 110 km since 1989 with an initial 75 m vertical resolution smoothed over 3 km. The total estimated error is less than 4 K and 8 K at the top and bottom of the profiles respectively, dropping to 0.6 K at mid-range (typically 90 km). At lower latitudes, the JPL Rayleigh/Raman lidars [*McDermid et al.*, 1995] located at TMF (34.4°N, 117.7°W) and MLO (44.0°N, 155.6°W) have obtained more than 685 and 410 temperature profiles from 30 to 80 km since 1988, and from 15 to 90 km since 1993 respectively. Most of the routine measurements comprise a 1.5-2.0 hour integration experiment, usually at the beginning of the night. The associated temperature errors are similar to those of the French Rayleigh lidars but the top of the profiles are slightly lowered.

For all instruments, each individual temperature profile was interpolated to obtain data points every one kilometer. Then, all temperature profiles were merged into a composite single year of data. A weighted running average with a triangular 33-day width filtering scheme was applied to each day of the composite year that a profile was available. No removal of tidal structures was performed. At MLO the role of the diurnal and semidiurnal tides may not be negligible above 80 km and similarly for the diurnal component at CSU above 90 km.

3. Results

a. Climatological temperatures.

The mean annual temperature climatologies obtained are presented in Figure 1(a) and (b) for OHP+CEL together (same latitude), and MLO. A distinctly defined temperature pattern is observed at both sites. For

OHP+CEL [Fig.1(a)] a familiar mid-latitude warm summer and cool winter stratosphere is observed with a maximum of 272 K in May-June and a minimum of 255 K in early November at the stratopause altitude of 47 km. A characteristic warm winter/cold summer mesosphere is also observed with a maximum of 220 K in December and January, and a minimum of 195-200 K in May-June at 75 km, which is in good agreement with previous climatologies [*Hauchecorne et al.*, 1991]. The weak negative vertical temperature gradient observed in winter is the consequence of the seasonal average of the so-called mesospheric temperature inversions occurring during the entire winter at OHP and CEL, and more specifically in February at TMF (not shown).

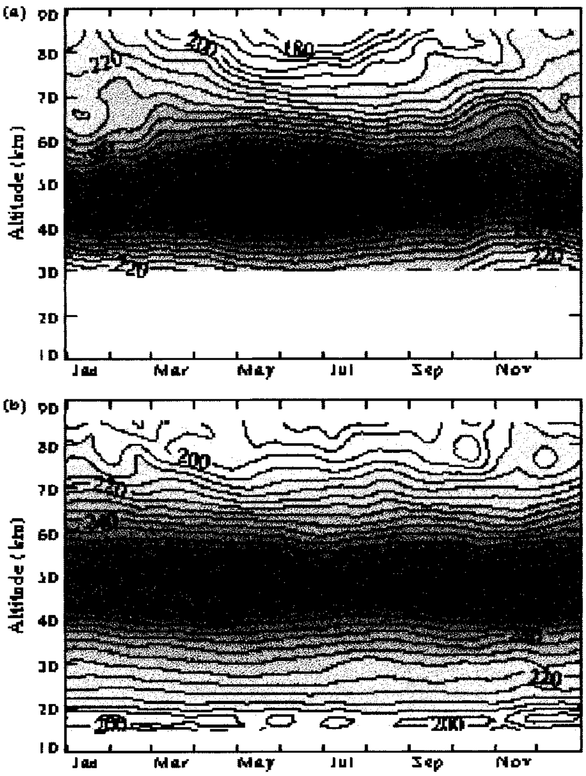

Figure 1. Climatological temperatures obtained from lidar measurements at (a) OHP+CEL (44.0°N), and (b) MLO (19.5°N, 155.6°W). Contour interval is 5 K.

Figure 1(b) (MLO) clearly shows a semiannual cycle at the stratopause and an annual cycle in the lower stratosphere with a very cold minimum of 190 K at 17 km identified as the tropical tropopause. As expected at these latitudes, the amplitude of the seasonal variations is weak. At the top (80-85 km), where the effect of the mesospheric tides is the largest, the measured cold temperatures are more representative of early night temperatures than nightly (or even a 24-hour) mean temperatures.

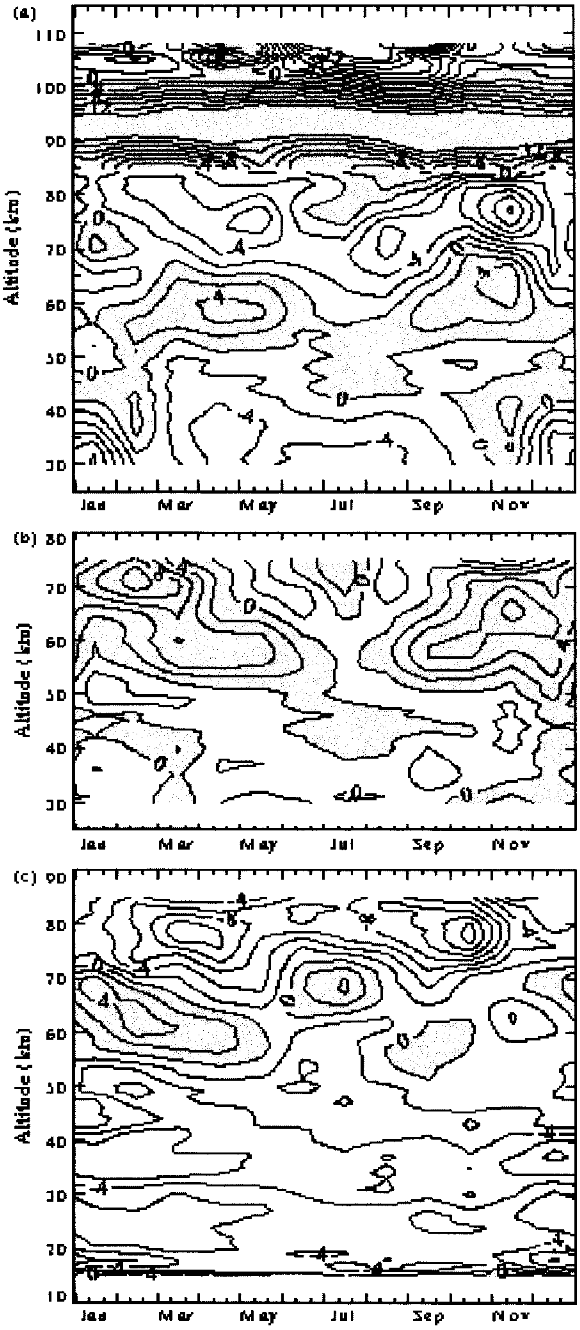

Figure 2. Monthly mean differences from the CIRA-86 temperatures for (a) OHP+CEL and CSU, (b) TMF, and (c) MLO. Contour interval is 2 K.

b. Difference from CIRA-86

The monthly mean lidar temperatures were subtracted from the monthly mean CIRA-86 temperatures [*Fleming et al.,* 1990]. The temperature difference between the observed lidar and the CIRA-86 climatologies is plotted in Figure 2(a) OHP+CEL and CSU, (b) TMF and (c) MLO. Since they have quasi-separated altitude ranges, OHP+CEL and CSU are presented on the same plot, Figure 2(a), with a separating altitude of 84-85 km.

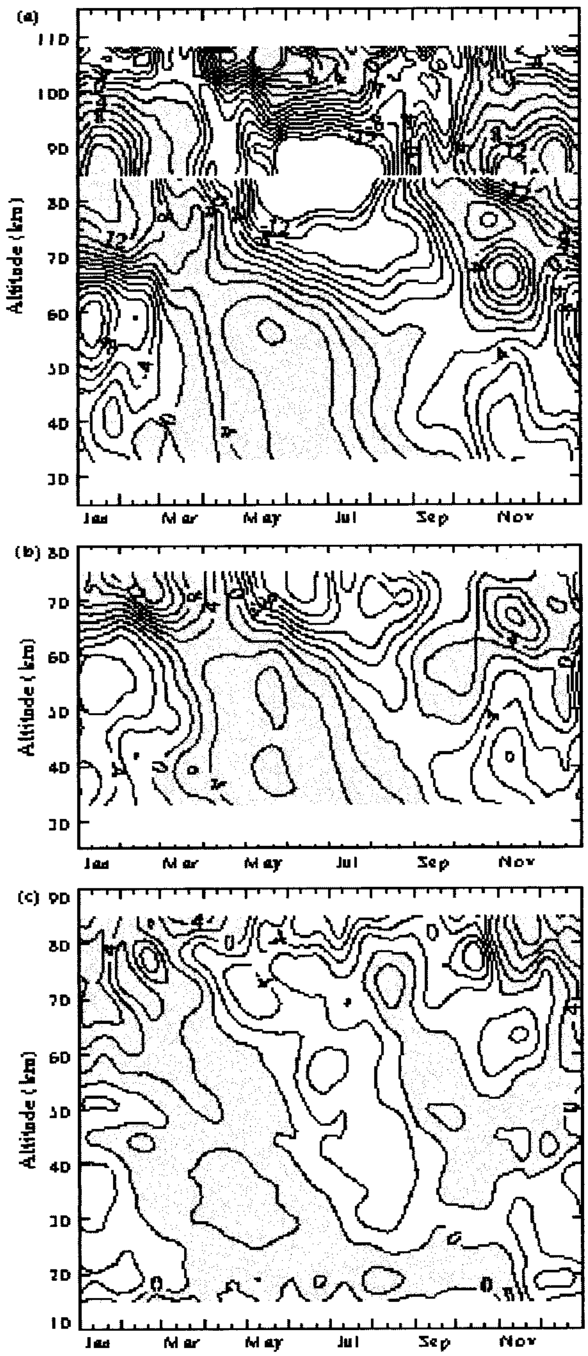

Figure 3. Daily mean deviation from the annual mean temperature (from the temperature climatology shown in Figure 1). (a) CSU and OHP+CEL, (b) TMF, (c) MLO. Contour interval is 2 K.

At OHP and CEL [Fig.2(a)] the observed temperatures are systematically 2-4 K colder than CIRA between 30 and 40 km, especially in summer, and 2-6 K colder between 70 and 80 km, while no systematic error is observed at stratopause altitudes. For MLO [Fig.2(c)] the entire region between 15 and 55 km is colder than the CIRA; up to 4 K in the upper stratosphere. In the stratosphere the systematic departure is about 2 K. At mesopause altitudes the systematic error is remarkably large at mid-latitudes as illustrated by the difference CSU-CIRA [Fig.2(a)] where a very large positive departure of more than 16 K is observed in the entire mesopause region (90-95 km). *Clancy et al.* [1994] reported similar SME/CIRA-86 departures suggesting that the CIRA is definitely too cold at these heights and latitudes.

In addition to the systematic errors, observed temperatures are up to 10 K colder than CIRA in December and January below 40 km at OHP+CEL. This can be explained by the out-of-phase occurrence, between late January and February, of stratospheric warmings at OHP and CEL and its equivalent occurring earlier in the CIRA model (December-January). Consequently the CIRA is too warm in December and January.

In the lower mesosphere OHP+CEL and TMF temperatures are warmer than CIRA. A maximum departure of 10 K near 70 km is observed in February at TMF, 4 K at 60 km in April-May for all mid-latitudes sites, and 4 K (respectively 8 K) at 60-70 km in November above OHP/CEL (respectively TMF). In the mid-mesosphere OHP/CEL temperatures are colder than CIRA with a maximum departure of 10 K in November at 75-80 km. At MLO [Fig.2(c)] the temperature departures are smaller than at mid- and subtropical-latitudes. This is not surprising since the variability is itself smaller at low-latitudes. Consequently the errors due to the annual and semi-annual amplitudes, and due to the seasonal transitions, are minimized. In the entire middle atmosphere the CIRA model is warmer except at two times of the year between 60 and 70 km. At 80 km a maximum negative departure of 10 K can be observed. In the 60-70 km region CIRA is colder as already observed at mid-latitudes [Fig.2(a),(b)]. Also, a very special pattern is observed at the beginning of the year; a negative departure is propagating downward from 80 km associated with a positive departure around 65 km and another negative departure between 50 and 55 km.

c. Temperature deviations from the annual mean

The annual mean temperature profile was then subtracted from each available daily composite profile to obtain the daily deviation from the annual mean. Figure 3 represents this deviation for (a) CSU and OHP+CEL, (b) TMF, and (c) MLO. As expected for CSU, OHP+CEL, and TMF [Fig.3(a),(b)] an annual cycle is clearly dominant in both the stratosphere and mesosphere. At 67-70 km its phase is inverted compared with the solar flux leading to the classic warm summer stratosphere and cold summer mesosphere and vice-versa in winter. A second phase inversion is clearly observed at CSU [Fig.3(a)] around 95-100 km, marking the transition between the dynamically and chemically or radiatively driven upper mesosphere. These plots, in particular Figure 3(a), also show a warm late-winter centered at 35-40 km. This is the signature of the stratospheric warmings occurring from January to March at mid- and high-latitudes. This signature is still observable in Figure 3(b) but with a weaker magnitude. Another warm spot is observed at 65-67 km in November reaching 11 K for OHP/CEL and 8 K for TMF. This feature can also be observed in Figure 1(a) as a bulge of warm temperatures in November between 60 and 70 km.

In contrast to the mid-latitudes sites MLO [Fig.3(c)] primarily exhibits a semi-annual cycle between 25 and 80 km altitude. This is not surprising since MLO is located at 19.5°N and is influenced by the equatorial dynamical pattern which in turn is affected by both northern and southern hemispheres. The semi-annual cycle observed here is almost a continuous downward propagating oscillation with an approximate vertical speed of 12 km/month and can be identified as the thermal semi-annual oscillation (SAO). The so-called mesopause and stratopause SAOs appear here as a combined single SAO propagating downward from the mesopause to 30 km with minimum amplitude at 45 km. A phase inversion is observed near 82 km similar to that observed by SME at 83 km [*Garcia and Clancy*, 1990]. The oscillation is strongly modulated with the first cycle being stronger than the second.

4. Summary

Long term measurements from several lidar instruments (Rayleigh/Raman and sodium) located at 44.0°N, 40.6°N, 34.4°N, and 19.5°N have been used to develop a new climatology of the middle atmosphere temperature. The climatologies for each lidar were first compared to the CIRA-86 model. Large differences between the lidar temperatures and the CIRA-86 temperatures are identified and explained. When compared to all instruments, CIRA-86 appears systematically too cold between 90 and 95 km, by 20 K or more, and possibly 6-8 K too warm around 80 km, making its use as a reference atmosphere model questionable at these altitudes. The annual and semi-annual components of the seasonal variability were investigated. An annual cycle with 6-7 K amplitude in the upper stratosphere, increasing to 15-20 K at 80 km, is observed at mid-latitudes. This cycle is in phase with the solar flux in the stratosphere and in opposite phase in the mesosphere with a very cold summer mesopause at 85 km, in good agreement with previous climatologies. At lower latitudes, a semiannual oscillation (SAO) propagates downward from 85 to 30 km and is characterized by a stronger first cycle than the second (4 K and 2 K amplitude respectively). Finally, sudden seasonal transitions, highly consistent between all instruments, have been observed (not shown here). In particular, in the early winter mid-latitudes a two-step warming of the winter mesosphere between 65 and 85 km as well as a cooling of the lower mesosphere appear to be real climatological events rather than some short-term geophysical or instrumental random variability.

Acknowledgements

The work described in this paper was carried out, in part, at the Jet Propulsion Laboratory, California Institute of Technology, under an agreement with the National Aeronautics and Space Administration.

References

Clancy, R. T., D. W. Rush, and M. T. Callan, Temperature minima in the average thermal structure of the middle atmosphere (70-80 km) from analysis of 40- to 92-km SME global temperature profiles, *J. Geophys. Res.*, *99*, 19,001-19,020, 1994.

Fleming, E. L., S. Chandra, J. J. Barnett and M. Corney, COSPAR International Reference Atmosphere, Chapter 2: Zonal mean temperature, pressure, zonal wind and geopotential height as functions of latitude, *Adv. Space Res.*, *10* (12), 11-59, 1990.

Garcia, R. R., and R. T. Clancy, Seasonal Variation in equatorial mesospheric temperatures observed by SME, *J. Atmos. Sci.*, *47*, 1666-1673, 1990.

Hauchecorne, A., and M. L. Chanin, Density and Temperature Profiles obtained by lidar between 35 and 70 km, *Geophys. Res. Lett.*, *7*, 565-568, 1980.

Hauchecorne, A., M. L. Chanin, and P. Keckhut, Climatology and trends of the middle atmospheric temperature (33-87 km) as seen by Rayleigh lidar over the south of France, *J. Geophys. Res.*, *96*, 15,297-15,309, 1991.

Leblanc, T., I. S. McDermid, A. Hauchecorne, and P. Keckhut, Evaluation and optimization of lidar temperature analysis algorithms using simulated data, JGR In Press, 1998.

McDermid, I. S., T. D. Walsh, A. Deslis and M. L. White, Optical systems design for a stratospheric lidar system, *Appl. Opt.*., *34*, 6201-6210, 1995.

She C. Y., J. R. Yu, H. Latifi, and R. E. Bills, High-spectral-resolution fluorescence light detection and ranging for mesospheric sodium temperature measurements, *Appl. Opt.*, *31*, 2095-2106, 1992.